Reports

Sequential Basal Faults in Devonian Dolomite, Nopah Range, Death Valley Area, California

Abstract. *Dolomite crystals from the Lost Burro Formation (Devonian) in the Nopah Range, eastern California, display basal stacking disorder as evidenced by transmission electron microscopy. Satellites in electron diffraction patterns indicate that stacking of anions and cations is different from that in ideal dolomite. This example conforms to the model of basal defects proposed by Goldsmith and Graf in 1958 to explain nonstoichiometry in dolomite. This dolomite from the Nopah Range was formed by deep burial replacement of micritic limestone, and its peculiar superstructure is tentatively attributed to the late diagenetic conditions during replacement.*

There is much evidence that many sedimentary carbonates which formed by replacement and neomorphism contain heterogeneous modulated structures. Modulations have been observed in calcian dolomite (*1*) but they are common in calcian and stoichiometric dolomites replacing Mg-calcite and dolomite (*2*) and in calcite neomorphic after Mg-calcite and aragonite (*3*). The modulations are parallel to the unit rhomb $r = \{10\bar{1}4\}$, have wavelengths from 200 to 2000 Å, and are more or less regular. Because of their occurrence in stoichiometric calcite, they were attributed (*4*) to disorder in the orientation of CO_3 groups, which, in ideal calcite, alternate regularly from one basal layer to the next. Disorder, it was proposed, was due to heterogeneities introduced by surface tensions, probability, and impurities in the solution during reprecipitation across a thin aqueous film in accord with the models of Land (*5*) and Sandberg (*6*). Heterogeneities apparent by contrast on electron micrographs were interpreted as stacking faults probably caused by disordered growth. If they are parallel to $\{10\bar{1}4\}$ they are conservative, that is, the fault vector $\mathbf{R} = \frac{2}{3}\mathbf{a}_1\ \frac{1}{3}\mathbf{a}_2\ \frac{1}{6}\mathbf{c}$ lies in the fault plane (Fig. 1a). Conservative faults do not change the composition of the material. However, nonconservative basal stacking faults with a displacement vector not in the fault plane (0001) (Fig. 1b) do cause a compositional change and were proposed to explain the nonstoichiometry of calcian dolomite as early as 1958 by Goldsmith and Graf (*7*).

Thus far, all observed modulated microstructures were parallel to $\{10\bar{1}4\}$, which cannot account for compositional variations (*2*), and Goldsmith and Graf's model remained hypothetical. Long-range ordered stacking variations have been documented in the series of rare earth carbonates (bastnaesite-roentgenite-synchisite) with both sequential and compositional faults (*8*). We have now found similar basal faults in unique dolomite crystals from the Nopah Range, east of Death Valley, California; these crystals formed by late diagenetic, deep burial replacement of very fine crystalline limestone (that is, micrite) in the Devonian Lost Burro Formation. Specifically, they are found in the transition zone of mixed carbonates between the lower, dolomitic part of the unit and the upper, dominantly limestone portion (*9*, *10*).

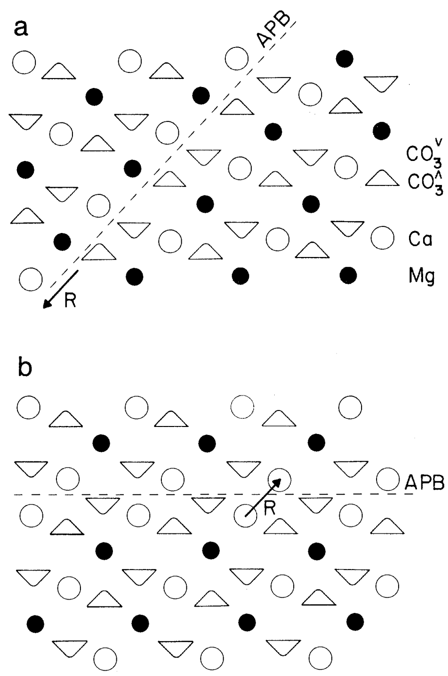

Fig. 1. $(11\bar{2}0)$ section of the structure of dolomite depicting layers of Ca, Mg, $CO_3^{\vee}$ (pointing backward), and $CO_3^{\wedge}$ (pointing forward) ions. A fault (in this case an antiphase boundary or APB) and the fault vector **R** are indicated. (a) Conservative APB; (b) nonconservative APB.

Shallow subtidal and peritidal carbonates in the lower Lost Burro have been pervasively dolomitized. Although direct indication of this may be lacking in many beds and samples, collective field and petrographic evidence, including dolomitized stromatoporoids and relict peloids, strongly suggest a replacement origin for most of the dolomite. Coarse crystallinity, zebroid structure, local facies changes between limestone and dolomite, dolomite tongues and fronts transecting limestone beds, and a "net fabric" indicate late diagenetic dolomitization (*10*). The general significance of burial dolomitization has been debated (*10–12*).

Net fabric involves the apparently unique dolomite crystals under discussion. Generally, it consists of seams of dolomite enclosing irregular, in places angular, millimeter- to decimeter-sized "cells" of micrite containing large (300 μm to 1 mm) rhombic, cross-shaped, dolomite crystals with undulatory extinction [Fig. 2 and (*13*)] which from all indications are replacing the calcite. There is a spectrum ranging from partial dolomitization along stylolites through an intermediate stage of typical net fabric to complete dolomitization exhibiting a relict fabric (Fig. 3). Truncation of stylolites, relict stylolites, and the overall geometry of the relict net fabric in the dolomite indicate that dolomitization occurred subsequent to initial pressure solution and was thus late diagenetic (*10*).

The euhedral cross-shaped crystals are most outstanding where they are disseminated in the micrite; however, cross-shaped terminations can also be distinguished against the micrite along the margins of the seams (Figs. 2 and 3). In the completely dolomitized equivalent, the cross-shaped outlines are lost in the process of compromise boundary development. Oxygen isotope data for these crystals [two samples: $\delta^{18}O$ (PDB) = −6.16 and −8.12] further support the idea of late diagenetic dolomitization in a deep burial environment subjected to temperatures well above those at or near the earth's surface.

After petrographic examination, areas in the specimen were selected for detailed analysis with the transmission electron microscope. Electron-transparent foils were prepared by ion beam thinning. A JEM 100 C microscope was used to characterize the microstructure with simultaneous x-ray analysis to verify the chemical composition.

The micrite matrix is fairly featureless. Calcite crystals, dominantly 3 to 4 μm in size, contain a few dislocations indicative of slight deformation. No twinning has been observed. Dolomite is easily recognized by a modulated microstructure which is pervasive throughout but not very homogeneous (Fig. 4). Modulations are generally parallel to $r = \{10\bar{1}4\}$ in accord with observations on other sedimentary carbonates. These modulations are not expressed in the diffraction pattern; in particular, no "c"-type superstructure reflections have been observed which characterize other dolomites with modulated structure (*2*). However, the diffraction pattern displays conspicuous diffuse streaking parallel to c^*, indicating disorder in the basal stacking. In addition, satellites appear about basic "a"-type reflections at a distance of one-third the spacing of a-type reflections along c^* (Fig. 5). They are the expression of a very fine periodic modulation along c which is different from the $\{10\bar{1}4\}$ structure. The additional reflections effectively increase the c lattice parameter three times in a new rhombohedral unit cell. The satellites about reflections hkl with l odd are particularly strong, and it is possible that those about l even are due to double diffraction, which is common in electron

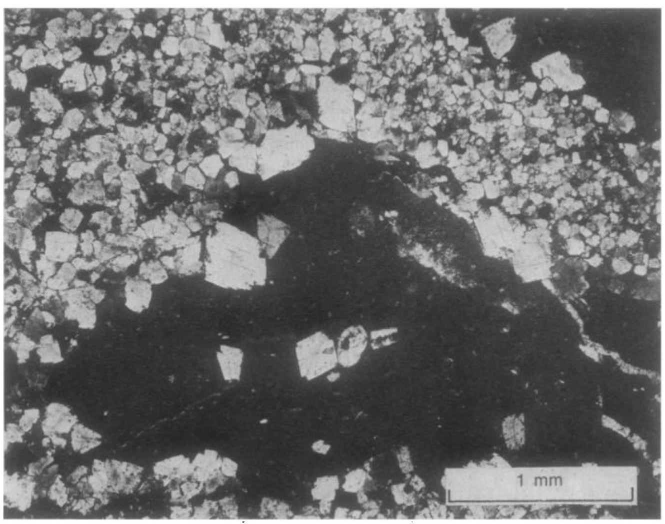

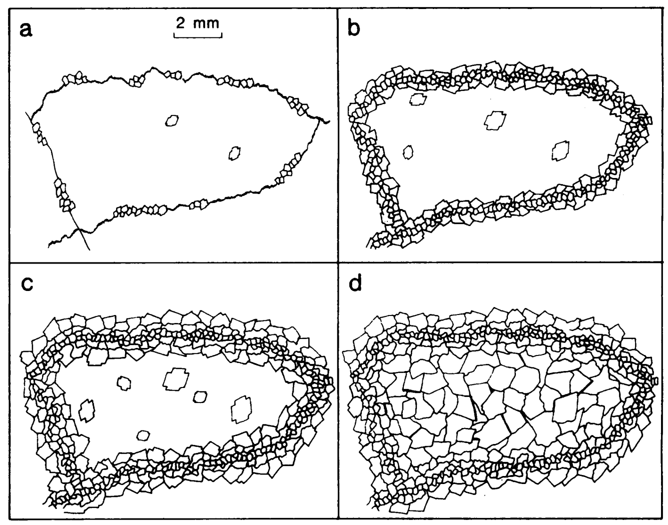

Fig. 2 (left). Photomicrograph of seams of dolomite crystals and unique, rhombic, cross-shaped dolomite crystals (light) in micritic limestone (dark); crossed polarizers. Fig. 3 (right). Model for the evolution of the net fabric (dolomite crystals outlined) beginning with (a) partial replacement along stylolites and in the pockets of calcite (blank areas, crystals not outlined) and ending with (d) complete replacement of micrite.

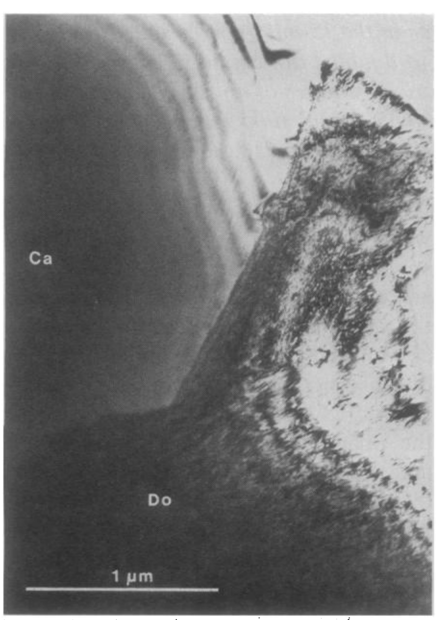

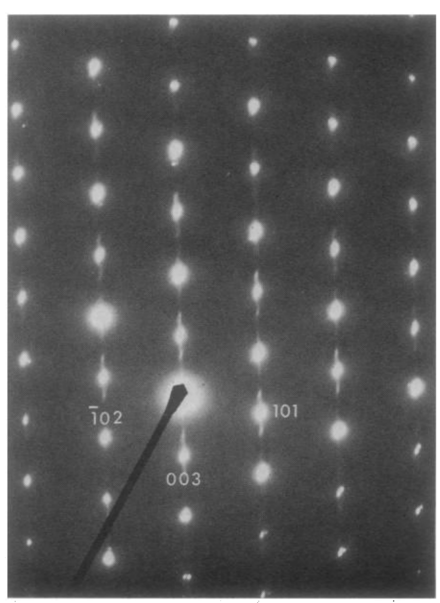

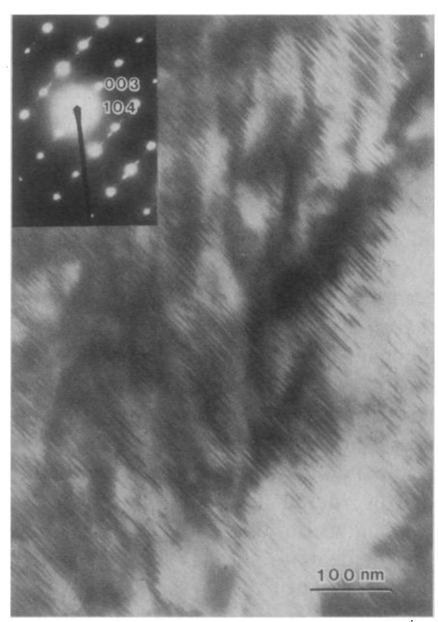

Fig. 4 (left). Bright-field electron micrograph of modulated microstructure in dolomite (*Do*) replacing calcite (*Ca*) and maintaining a straight interface parallel to $r = \{10\bar{1}4\}$. The modulation, in contrast, is parallel to $r = \{\bar{1}104\}$. Fig. 5 (middle). Diffraction patterns displaying streaking parallel to c^* and satellites indicative of a new dolomite superstructure. Note that satellites about reflections with l odd are particularly strong. Fig. 6 (right). Dark-field electron micrograph imaged with a pair of strong satellites operating. They show fringes parallel to (0001), which are interpreted as more or less periodic nonconservative antiphase boundaries. The dark and light elongated domains are attributed to the $\{10\bar{1}4\}$ modulated structure (the inset diffraction pattern documents the crystallographic orientation of the defects).

diffraction. The two satellites on either side of an a-type reflection have similar intensity.

With reflections which have strong satellites, sharp quasi-periodic boundaries parallel to (0001) are in good contrast in dark-field micrographs (Fig. 6). The boundaries, spaced at 30 Å (corresponding to the distance between the two satellites), are disrupted across the $\{10\bar{1}4\}$ structure, which appears as diffuse dark and light regions. Streaking parallel to c^* indicates that faults are not strictly periodic, which is evident from the morphology of the pattern.

The occurrence of satellites in the diffraction pattern of dolomite documents a new superstructure in this mineral. The superstructure contains a basal stacking which is different from that of ideal dolomite and the faults imaged in Fig. 6 could represent periodic antiphase domain boundaries (APB) with a morphology very similar to that of metamorphic intermediate plagioclase (*14*). Nonconservative APB's can be due to cation ordering from a disordered state, but in the case of dolomite it is more likely that they formed during replacement growth. They appear to be an expression of nonstoichiometry with extra layers of Ca intercalated in the structure (*7*). In fact, the crystals under consideration are Ca-rich ($Ca_{0.54}Mg_{0.46}CO_3$) as determined by microprobe analysis. Other possibilities are a different stacking of anion layers or a combination of cation and anion stacking. At this stage the evidence is insufficient to identify the true structure and we must await results from high-resolution microscopy.

The basal stacking superstructure has been found in all crystals in the net fabric, both in euhedral crystals growing in the calcite cells and in the subhedral crystals in the seams evolving from replacement along stylolites. It is present equally in all stages of replacement, including samples in which dolomite has completely replaced calcite, suggesting that physicochemical conditions and mechanisms of dolomitization were similar throughout. It appears that basal defects represent structures formed during deep burial replacement and that the original dolomite structure was probably not disordered "protodolomite" (*15, 16*) but contains a different type of ordering than "ideal" dolomite. The prominent growth form of the dolomite crystals in the studied samples is $r = \{10\bar{1}4\}$. The Lost Burro crystals also provide a clear example of late diagenetic replacement of consolidated limestone, both along stylolites and directly in the matrix.

Locally, Mg must have migrated to the site of nucleation along stylolites, now-healed microfractures, and crystal boundaries. The unique occurrence, morphology, and microstructure of these samples add complexity to the "dolomite problem" (*17, 18*) and encourage more systematic surveys of sedimentary dolomites with the transmission electron microscope. Heretofore, little has been done in this regard, and most of the work has been on low-temperature dolomites (*1, 2*). Specifically, the geologic significance of the new dolomite superstructure needs to be explored to determine more precisely the conditions leading to its formation. We have begun to study the extent of dolomite with satellites in the Lost Burro Formation away from the limestone-dolomite contacts. Such study bears on the questions of pervasiveness and operating mechanisms of burial dolomitization.

H. R. Wenk
Department of Geology and Geophysics, University of California, Berkeley 94720

D. H. Zenger
Department of Geology, Pomona College, Claremont, California 91711

References and Notes

1. R. J. Reeder and H. R. Wenk, *Geophys. Res. Lett.* **6**, 77 (1979).
2. R. J. Reeder, *Contrib. Mineral. Petrol.* **76**, 148 (1981).
3. S. H. Gunderson and H. R. Wenk, *Am. Mineral.* **66**, 789 (1981).
4. H. R. Wenk and S. Frisia-Bruni, *Geol. Soc. Am. Abstr. Programs 14* (No. 7) (1982).
5. L. S. Land, *Sedimentology* **20**, 411 (1973).
6. P. A. Sandberg, *ibid.* **22**, 495 (1975).
7. J. R. Goldsmith and D. L. Graf, *Am. Mineral.* **43**, 84 (1958).
8. J. Van Landuyt and S. Amelinckx, *ibid.* **60**, 351 (1975).
9. D. H. Zenger, in *Geology of Selected Areas in the San Bernardino Mountains, Western Mojave Desert, and Southern Great Basin, California: Guidebook and Volume, Field Trip 9, Cordilleran Section*, J. D. Cooper, B. W. Troxel, L. A. Wright, Eds. (Cordilleran Section Meeting, Geological Society of America, Anaheim, Calif., 1982), pp. 129–136.
10. D. H. Zenger, *Geology*, in press.
11. B. W. Mattes and E. W. Mountjoy, *Soc. Econ. Paleontol. Mineral. Spec. Publ. 28* (1980), pp. 259–297.
12. D. W. Morrow, *Geosci. Can.* **9**, 95 (1982).
13. Cover page, *Am. Assoc. Pet. Geol. Bull.* 66 (No. 1) (1982).
14. H. R. Wenk and Y. Nakajima, *Phys. Chem. Miner.* **6**, 169 (1980).
15. A. M. Gaines, *Science* **183**, 518 (1974).
16. D. L. Graf and J. R. Goldsmith, *J. Geol.* **64**, 173 (1956).
17. R. W. Fairbridge, "Regional aspects of carbonate deposition," *Soc. Econ. Paleontol. Mineral. Spec. Publ. 5* (1957), pp. 124–178.
18. G. V. Chilingar, D. H. Zenger, H. J. Bissell, K. H. Wolf, *Dev. Sedimentol.* **25A**, 423 (1979).
19. Supported by NSF grant 7823848 (to H.R.W.) and American Chemical Society, Petroleum Research Fund, grants 13615-AC2 (to H.R.W.) and 2678-B2 (to D.H.Z.).

20 October 1982; accepted 17 June 1983

Satellite Detection of Effects Due to Increased Atmospheric Carbon Dioxide

Abstract. *The use of satellites to detect climatic changes due to increased carbon dioxide was investigated. This method has several advantages over ground-based methods of monitoring climatic change. Calculations indicate that, by monitoring the outgoing longwave flux for small intervals in the 15-micrometer spectral region, changes in stratospheric temperatures due to doubled atmospheric carbon dioxide are large enough to be detected above the various sources of noise. This method can be extended to other spectral regions so that causal links between changes in outgoing longwave radiation due to other trace gases and the thermal structure of the atmosphere could be established.*

Various methods have recently been proposed to detect a climatic signal due to increased atmospheric CO_2 (*1*). Most of these methods involve studying surface climatic variables (surface temperature, sea levels, area of ice coverage, and so forth), which are strongly affected by a myriad of atmospheric, oceanic, and cryospheric processes. The methods cannot establish any causal connection between observed changes in a climatic variable and changes in the radiative balance of the earth-atmosphere system, and they are limited in their spatial and temporal coverage, which in turn limits the sample size used to determine a climatic change.

One climatic variable that is easily measured on a global scale is the longwave flux emitted at the top of the atmosphere. The amount of energy emitted at any given spectral interval depends on the atmospheric temperature structure as well as on the amount and distribution of absorbers. Any increase in atmospheric CO_2 will lead to an increase in the opacity of the earth's atmosphere and thus to an alteration in the spectral distribution of outgoing energy (*2*).

To estimate the magnitude of this change in a selected spectral region, we performed a series of calculations to determine the outgoing flux of energy in the 500 to 800 cm^{-1} spectral region. This region, centered around 15 μm, contains the CO_2 band system that is most important for studies of increased CO_2. Most of the emission of longwave radiation